bioRxiv preprint doi: https://doi.org/10.1101/182444; this version posted August 30, 2017. The copyright holder for this preprint (which was not certified by peer review) is the author/funder, who has granted bioRxiv a license to display the preprint in perpetuity. It is made available under aCC-BY 4.0 International license.

The modulation of neural gain facilitates a transition between functional segregation and integration in the brain

Authors

James M. Shine[1,2*], Matthew J. Aburn[3], Michael Breakspear[3,4] and Russell A. Poldrack[1]

Affiliations

1 – Department of Psychology, Stanford University, Stanford, CA, USA

2 – Neuroscience Research Australia, The University of New South Wales, Sydney, Australia

3 – QIMR Berghofer Medical Research Institute, Brisbane, Australia

4 – Metro North Mental Health Service, Brisbane, QLD, Australia

bioRxiv preprint doi: https://doi.org/10.1101/182444; this version posted August 30, 2017. The copyright holder for this preprint (which was not certified by peer review) is the author/funder, who has granted bioRxiv a license to display the preprint in perpetuity. It is made available under aCC-BY 4.0 International license.

Abstract

Cognitive function relies on a dynamic, context-sensitive balance between functional integration and segregation in the brain. Previous work has proposed that this balance is mediated by global fluctuations in neural gain by projections from ascending neuromodulatory nuclei. To test this hypothesis *in silico*, we studied the effects of neural gain on network dynamics in a model of large-scale neuronal dynamics. We found that increases in neural gain pushed the network through an abrupt dynamical transition, leading to an integrated network topology that was maximal in frontoparietal 'rich club' regions. This gain-mediated transition was also associated with increased topological complexity, as well as increased variability in time-resolved topological structure, further highlighting the potential computational benefits of the gain-mediated network transition. These results support the hypothesis that neural gain modulation has the computational capacity to mediate the balance between integration and segregation in the brain.

bioRxiv preprint doi: https://doi.org/10.1101/182444; this version posted August 30, 2017. The copyright holder for this preprint (which was not certified by peer review) is the author/funder, who has granted bioRxiv a license to display the preprint in perpetuity. It is made available under aCC-BY 4.0 International license.

The function of complex networks such as the human brain requires a trade-off between functional specialization and global communication (Deco et al., 2015a; Park and Friston, 2013; Tononi and Sporns, 1994). Contemporary models of brain function suggest that this balance is manifest through dynamically changing patterns of correlated activity, constrained by the brains' structural backbone (Deco et al., 2013; Honey et al., 2007; Varela et al., 2001). This in turn allows exploration of a repertoire of cortical states that balance the opposing topological properties of segregation (i.e. modular architectures with high functional specialization) and integration (i.e. inter-connection between specialist regions; Deco et al., 2015b; Ghosh et al., 2008).

Recent work has demonstrated that the extent of integration in the brain is important for a range of cognitive functions, including effective task performance (Bassett et al., 2015; Shine et al., 2016a), episodic memory retrieval (Westphal et al., 2017) and conscious awareness (Barttfeld et al., 2015; Godwin et al., 2015). Furthermore, the topological properties of functional brain networks have been shown to fluctuate over time (Chang and Glover, 2010; Hutchison et al., 2013), both within individual neuroimaging sessions (Shine et al., 2016a; Zalesky et al., 2014) and over the course of weeks to months (Shine et al., 2016b). While the extent of integration in the brain may relate to more effective inter-regional communication, perhaps via synchronous oscillatory activity (Fries, 2015; Lisman and Jensen, 2013; Varela et al., 2001), there are also benefits related to a relatively segregated network architecture, including lower metabolic costs (Bullmore and Sporns, 2012; Zalesky et al., 2014) and effective performance as a function of learning (Bassett et al., 2015). However, despite these insights, the biological mechanisms responsible for driving fluctuations between integration and segregation remain unclear.

A candidate mechanism underlying flexible brain network dynamics is the global alteration in neural gain mediated by ascending neuromodulatory nuclei such as the locus coeruleus (Aston-Jones and Cohen, 2005a; Sara, 2009). This small pontine nucleus projects diffusely throughout the brain and releases noradrenaline, a potent modulatory neurotransmitter that alters the precision and responsivity of targeted neurons (Waterhouse et al., 1988). Alterations in this system are known to play a crucial role in cognition, as there is evidence for a

bioRxiv preprint doi: https://doi.org/10.1101/182444; this version posted August 30, 2017. The copyright holder for this preprint (which was not certified by peer review) is the author/funder, who has granted bioRxiv a license to display the preprint in perpetuity. It is made available under aCC-BY 4.0 International license.

nonlinear (inverted-U shaped) relationship between noradrenaline concentration and cognitive performance (Robbins and Arnsten, 2009; Figure 1a).

Mechanistically, the noradrenergic system has been shown to alter neural gain (Servan-Schreiber et al., 1990; Figure 1b), increasing the signal to noise ratio of afferent input onto regions targeted by projections from the locus coeruleus. A crucial question is how these local changes in neural gain influence the configuration of the brain at the network level. Recent work has linked fluctuations in network topology to changes in pupil diameter (Eldar et al., 2013; Shine et al., 2016a), an indirect measure of locus coeruleus activity (Joshi et al., 2016; Murphy et al., 2014; Reimer et al., 2014; 2016), providing evidence for a link between the noradrenergic system and network-level topology. However, despite these insights, the mechanisms through which alterations in neural gain mediate fluctuations in global network topology are poorly understood.

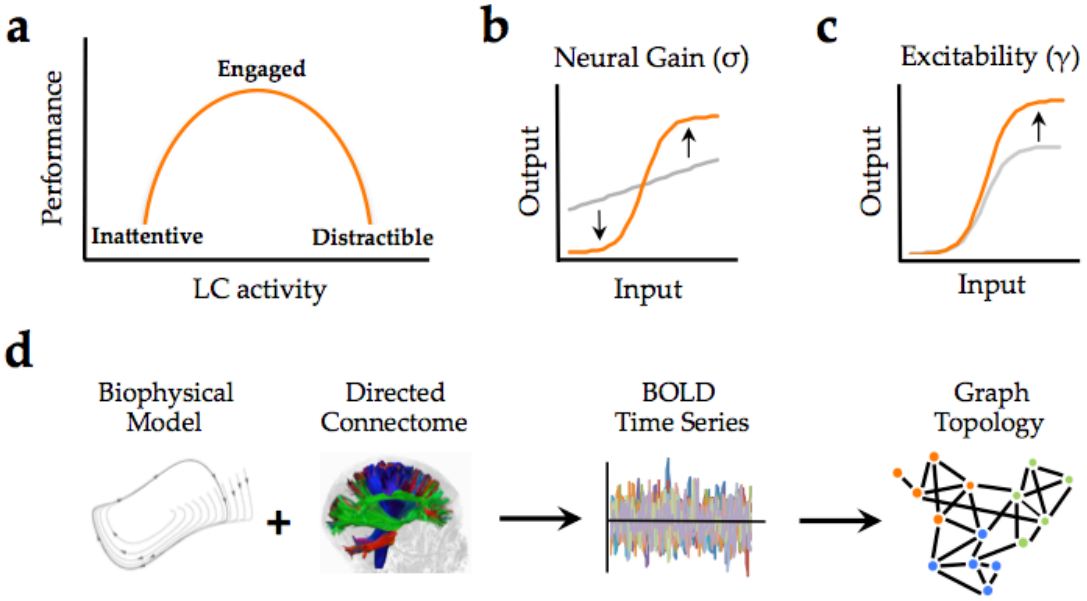

Figure 1 – Manipulating Neural Gain: a) the Yerkes-Dodson relationship linking activity in the locus coeruleus nucleus to cognitive performance; b) neural gain is modeled by a parameter (σ) that increases the maximum slope of the transfer function between incoming and outgoing activity within a brain region; c) excitability is modeled by a parameter (γ) that amplifies the level of output; d) the approach presently used to estimate network topology from the biophysical model.

bioRxiv preprint doi: https://doi.org/10.1101/182444; this version posted August 30, 2017. The copyright holder for this preprint (which was not certified by peer review) is the author/funder, who has granted bioRxiv a license to display the preprint in perpetuity. It is made available under aCC-BY 4.0 International license.

Biophysical models of large-scale neuronal activity have yielded numerous insights into the dynamics of brain function, both during the resting state as well as in the context of task-driven brain function (Deco et al., 2009; Honey et al., 2007) (for review, see Breakspear, 2017). Whereas prior research in this area has examined the influence of local dynamics, coupling strength, structural network topology and stochastic fluctuations on functional network topology (Deco et al., 2015b; Deco and Jirsa, 2012; Deco et al., 2017; Gollo et al., 2015; Woolrich and Stephan, 2013), the direct influence of neural gain has not been studied. Here, we used a combination of biophysical modeling and graph theoretical analyses (Sporns, 2013) to characterize the effect of neural gain on emergent network topology. Based on previous work (Shine et al., 2016a), we hypothesized that manipulations of neural gain would modulate the extent of integration in time-averaged patterns of functional connectivity.

Results

To test this hypothesis, we implemented a generic 2-dimensional neuronal oscillator model (Fitzhugh, 1961; Stefanescu and Jirsa, 2011) within the Virtual Brain toolbox (Jirsa et al., 2010; Sanz Leon et al., 2013) to generate regional time series that were constrained by a directed white matter connectome derived from the CoCoMac database (Kötter, 2004; Figure 1d). The simulated neuronal time series were passed through a Balloon-Windkessel model to simulate realistic BOLD data. Graph theoretical analyses were then applied to time-averaged correlations of regional BOLD data to estimate the functional topological signatures of network fluctuations (see Methods for further details).

To simulate the effect of ascending neuromodulatory effects on inter-regional dynamics, we systematically manipulated neural gain (σ; Figure 1b) and excitability (γ; Figure 1c). These two parameters alter different aspects of a sigmoidal transfer function, which models the nonlinear relationship between presynaptic afferent inputs and local firing rates (Freeman, 1979). When the σ and γ parameters are both low, fluctuations in regional activity arise mainly due to noise and local feedback. As the σ and γ parameters increase, the influence of activity communicated from connected input regions also increases, leading to non-linear cross-talk and hence, changes in global brain topology and dynamics. Here, we investigated the topological signature of simulated BOLD time series

bioRxiv preprint doi: https://doi.org/10.1101/182444; this version posted August 30, 2017. The copyright holder for this preprint (which was not certified by peer review) is the author/funder, who has granted bioRxiv a license to display the preprint in perpetuity. It is made available under aCC-BY 4.0 International license.

across a parameter space spanned by σ and γ in order to understand the combined effect of neural gain and excitability on global brain network dynamics.

Neural gain and excitability modulate network-level topological integration

We simulated BOLD time series data across a range of σ (0-1) and γ (0-1) and then subjected the time series from our simulation to graph theoretical analyses (Rubinov and Sporns, 2010). This allowed us to estimate the amount of integration (quantified using mean participation coefficient; B_A) in the time-averaged functional connectivity matrix across the parameter space (Figure 2a). After excluding aspects of the parameter space that were associated with a poor correspondence between functional and structural connectivity matrices ($r < 0.2$; grey zones in Figure 2a), we observed a complex relationship between σ, γ and B_A, such that maximal integration occurred at high levels of σ but with intermediate values of γ. Outside of this zone, the time-averaged connectome was markedly less integrated.

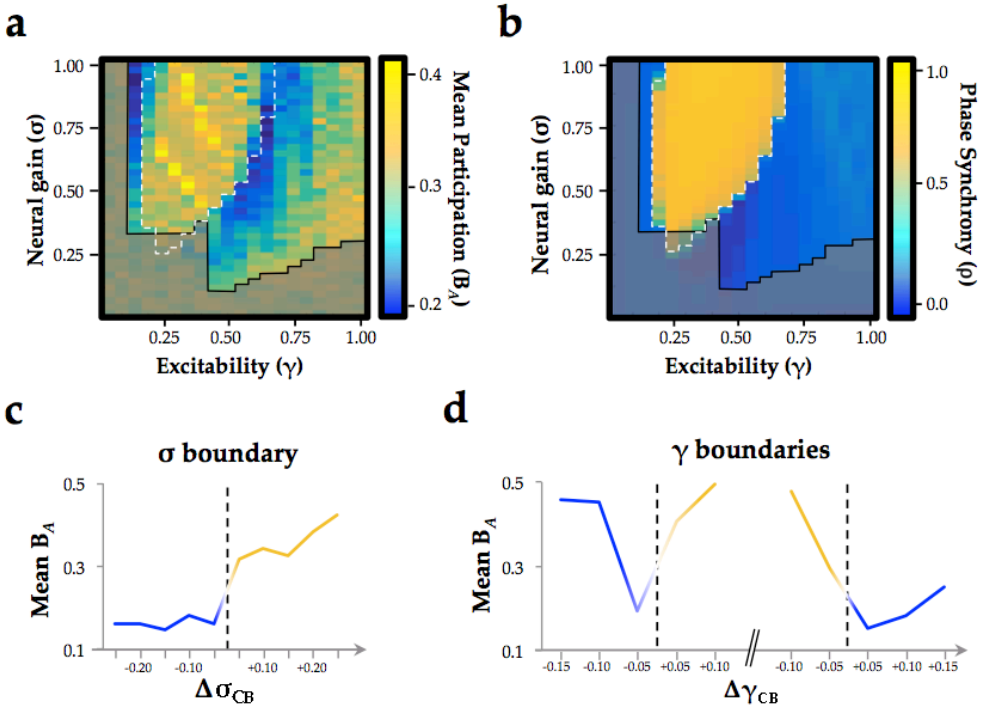

Figure 2 – a) mean participation as a function of σ and γ – greyed-out zones reflect parameter combinations that led to substantial differences between the functional and structural connectome ($r < 0.2$); b) phase synchrony (ρ) as a function of σ and γ; c): mean participation (B_A) aligned to the critical point (represented here as a dotted line) as a function of increasing σ; d) B_A aligned to the critical point as a function of increasing γ – the left and right dotted lines depicts

bioRxiv preprint doi: https://doi.org/10.1101/182444; this version posted August 30, 2017. The copyright holder for this preprint (which was not certified by peer review) is the author/funder, who has granted bioRxiv a license to display the preprint in perpetuity. It is made available under aCC-BY 4.0 International license.

the synchrony change at low and high γ, respectively. The *y*-axis in c) and d) represents the distance in parameter space aligned to the critical point/bifurcation for either σ ($\Delta\sigma_{CB}$; mean across $0.2 \leq \gamma \leq 0.6$) or γ ($\Delta\gamma_{CB}$; mean across $0.3 \leq \sigma \leq 1.0$). Lines are colored according to the state of phase synchrony on either side of the bifurcation (blue: low synchrony; yellow: high synchrony).

Neural gain transitions the network across a critical boundary

The relative simplicity of our local neural model allows formal quantification of the inter-regional phase relationships that characterize the underlying neuronal dynamics. These fast neuronal phase dynamics compliment the view given by the slow BOLD amplitude fluctuations and give insight into their fundamental dynamic causes. We employed a phase order parameter, that quantifies the extent to which regions within the network align their oscillatory phase – high values on this scale reflect highly ordered synchronous oscillations across the network, whereas low values reflect a relatively asynchronous system (Breakspear and Heitmann, 2010; Kuramoto, 1984).

Across the parameter space, we observed two clear states (Figure 2b): one associated with high ($\rho \geq 0.5$; yellow) and one with low ($\rho < 0.5$; blue) mean synchrony, with a clear critical boundary demarcating the two states (dotted white line in Figure 2a/b). This strong demarcation between states is a known signature of critical behavior (Chialvo, 2010), which can occur at both the regional and network level. We observed evidence for both regional and network criticality in our simulation, whereby small changes in parameters (here, σ and γ) facilitated an abrupt transition between qualitatively distinct states. At the regional level, this pattern is observed as a transition from input-driven fluctuations about a stable equilibrium to self-sustained oscillations (Figure S1). At the network level, the combined influence of increased gain and structural connections manifest as a transition to high amplitude, inter-regional phase synchrony (Figure 2b).

A host of contemporary neuroscientific theories hypothesize that temporal phase synchrony between regions underlies effective communication between neural regions (Fries, 2015; Lisman and Jensen, 2013; Varela et al., 2001), which would otherwise remain isolated if not brought into temporal lockstep with one another. As such, we might expect that the changes in neural gain that integrate

bioRxiv preprint doi: https://doi.org/10.1101/182444; this version posted August 30, 2017. The copyright holder for this preprint (which was not certified by peer review) is the author/funder, who has granted bioRxiv a license to display the preprint in perpetuity. It is made available under aCC-BY 4.0 International license.

the brain might do so through the modulation of inter-regional phase synchrony. Our results were consistent with this hypothesis. By aligning changes in the topological signature of the network to the critical point delineating the two states, we were able to demonstrate a significant increase in integration (mean B_A; $T_{798} = 2.57$; $p = 0.01$) and decrease in segregation (Q; $T_{798} = -17.44$; $p < 0.001$) of network-level BOLD fluctuations in the highly phase synchronous state. Specifically, global integration demonstrated a sharp increase in the zone associated with the high amplitude synchronous oscillations, particularly for intermediate values of γ (Figure 2c). In contrast, the transitions associated with manipulating γ (particularly at high values of σ) led to an inverse U-shaped relationship: the network was relatively segregated at high and low levels of γ, but integrated at intermediate values of γ (Figure 2d). In addition, increases in between-hemisphere connectivity were more pronounced than within-hemisphere connectivity in the ordered state (within: 0.010 ± 0.017; between: 0.014 ± 0.013; $T_{2,848} = 7.104$; $p = 10^{-12}$; see Figure S2). Together, these results suggest that neural gain and excitability act together to traverse a transition in network dynamics, maximizing inter-regional phase synchrony and integrating the functional connectome.

Neural gain increases topological complexity and temporal variability

Having identified a relationship between neural gain and network architecture, we next investigated the putative topological benefit of this trade-off. A measure that characterizes the topological balance between integration and segregation is communicability (Estrada and Hatano, 2008), which quantifies the number of short paths that can be traversed between two regions of a network (Mišić et al., 2015). In networks with high communicability, individual regions are able to interact with a large proportion of the network through relatively short paths, which in turn may facilitate effective communication between otherwise segregated regions. In contrast to the relationship observed between neural gain and network integration, communicability was maximal at the critical boundaries between synchronous and asynchronous behavior (Figure 3a-c). Thus, the topological signature of the network was most effectively balanced between integration and segregation as the system transitioned between disorder and order through the modulation of inter-regional synchrony by subtle changes in neural gain.

bioRxiv preprint doi: https://doi.org/10.1101/182444; this version posted August 30, 2017. The copyright holder for this preprint (which was not certified by peer review) is the author/funder, who has granted bioRxiv a license to display the preprint in perpetuity. It is made available under aCC-BY 4.0 International license.

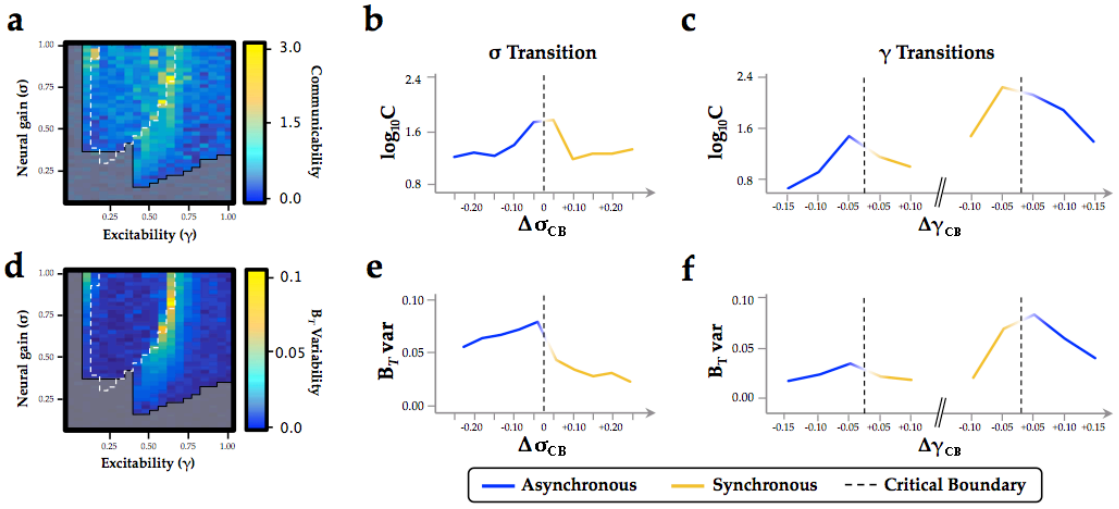

Figure 3 – Topological and temporal relationships with phase regimen boundary: a-c) network communicability was maximal following the σ boundary ($\Delta\sigma_{CP}$; mean across $0.2 \leq \gamma \leq 0.6$) and the immediately prior to the abrupt phase transition at high γ ($\Delta\gamma_{CP}$; mean across $0.3 \leq \sigma \leq 1.0$); d-f) time-resolved between-module participation (B_T) was maximally variable with increasing σ and across the critical boundary at high γ.

Another important signature of complex systems is their flexibility over time. In previous work, we showed that the 'resting state' is characterized by significant fluctuations in network topology, in which the brain traverses between states that maximize either integration or segregation (Shine et al., 2016a). This variability was diminished during a cognitively challenging task, and the extent of integration was positively associated with improved task performance (Shine et al., 2016a). To determine whether these alterations in topological variability may have been related to changes in neural gain, we estimated the time-resolved mean participation coefficient (B_T) of the simulated BOLD time series and then determined whether the variability of this measure over time changed as a function of σ and γ. We found that the variability of time-resolved integration within each trial was maximized across the critical boundary, as the network switched between disordered and ordered phase synchrony (Figure 3d-f). These results support the hypothesis that changes in neural gain may control the temporal variability of network topology as a function of behavioral state.

bioRxiv preprint doi: https://doi.org/10.1101/182444; this version posted August 30, 2017. The copyright holder for this preprint (which was not certified by peer review) is the author/funder, who has granted bioRxiv a license to display the preprint in perpetuity. It is made available under aCC-BY 4.0 International license.

Gain-mediated integration is maximal in frontoparietal hub regions

To determine whether the influence of neural gain on network dynamics was related to the underlying structural connectivity of the brain, we estimated the "rich club" architecture of the structural connectome (Figure 4a). Compared to low-degree nodes, rich club regions demonstrated an increase in 'realized' mean gain adjacent to the critical boundary (Figure 4b). In short, this means that activity within frontoparietal 'hub' regions (red in Figure 4a) was more strongly affected by the interaction between neural gain and network topology than in non-hub regions (blue/green in Figure 4a). Indeed, this result demonstrates that the 'realized' gain of individual regions is not simply related to the applied gain (i.e. input from the ascending noradrenergic system; Aston-Jones and Cohen, 2005b), but also non-linearly depends on afferent activity from topologically connected regions (Figure 4c/d). The observed effect was particularly evident for intermediate values of γ, suggesting that the hub regions were differentially impacted by neural gain at the critical boundary between the asynchronous and synchronous states. Together, these results confirm a crucial role for frontoparietal regions in the control of network-level integration as a function of ascending neuromodulatory gain.

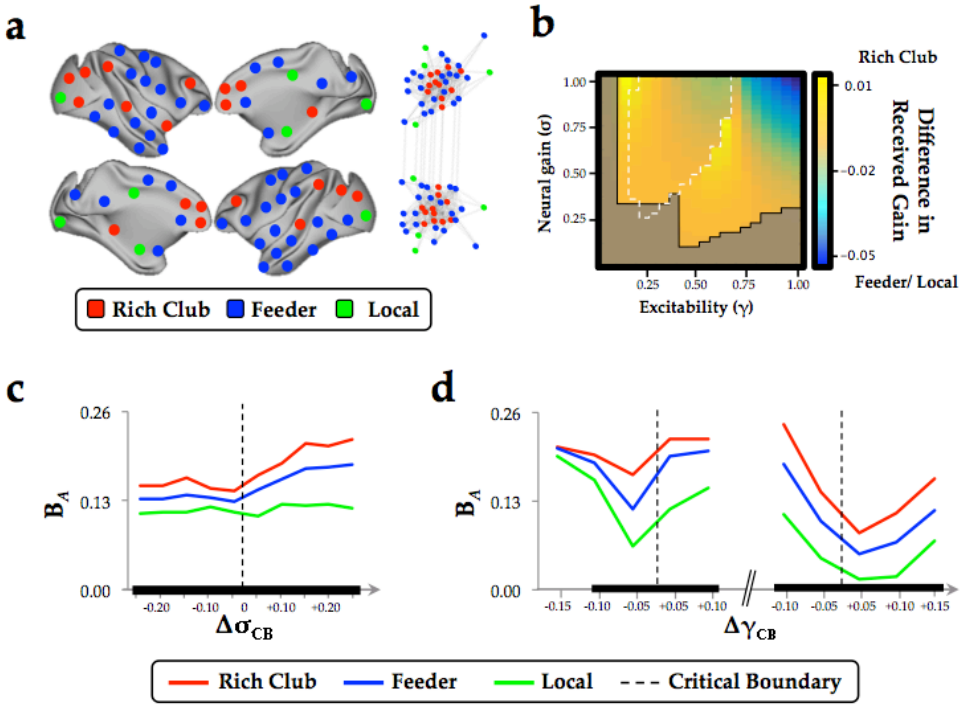

Figure 4 – Regional clustering results: a) regions from the CoCoMac data organized according to rich club (red), feeder (blue) or local (green) status, along with a force-directed plot of the top 10% of connections (aligned by hemisphere), colored according to structural hub connectivity status;

bioRxiv preprint doi: https://doi.org/10.1101/182444; this version posted August 30, 2017. The copyright holder for this preprint (which was not certified by peer review) is the author/funder, who has granted bioRxiv a license to display the preprint in perpetuity. It is made available under aCC-BY 4.0 International license.

b) the rich club cluster demonstrated an increase in realized mean gain (the relative output as a function of its' unique topology) at the bifurcation boundary, compared to feeder and local nodes, which showed higher realized gain at high levels of σ and γ; c) the three clusters of regions also demonstrated differential responses to neural gain; and d) excitability. The black lines in c) and d) denote significant differences in B_A between the two groups.

Discussion

We used a combination of computational modeling and graph theoretical analyses, quantifying the relationship between ascending neuromodulation and network-level integration in order to test a direct prediction from a previous neuroimaging study (Shine et al., 2016a). We found that increasing neural gain transitioned network dynamics across a bifurcation from disordered to ordered phase synchrony (Figure 2b) with a shift from a segregated to integrated neural architecture (Figure 2e). The critical boundary between these two states was associated with maximal communicability and temporal topological variability (Figure 3). Finally, the effect of neural gain was felt most prominently in high-degree frontoparietal network hubs (Figure 4). Together, these results confirm our prior hypothesis and complement an emerging view of the brain that highlights a mechanistic bridge between ascending arousal systems and cognition (Shine et al., 2016a), providing a potential mechanistic explanation for the long-standing notion that noradrenergic activity demonstrates an inverted U-shaped curve with cognitive performance (Robbins and Arnsten, 2009; Figure 1a).

The major result from our study is that network-level fluctuations between segregation and integration in functional (BOLD) networks reflect an underlying transition in synchrony of faster neuronal oscillations, thus providing a previously unknown link between temporal scales in the brain (Figure 2b). At low levels of γ and σ, the governing equations are strongly stable (damped), so that all excursions from equilibrium must be driven by local noise – that is, regions are relatively insensitive to incoming inputs (Figure 1b/c). As γ and σ increase, local activity approaches an instability, and consequently incoming activity is able to substantially influence activity in target regions. This causes changes in the emergent whole-brain dynamics evident at both the short time scale of brain oscillations and the long time scale of BOLD correlation. A stark transition occurs at a critical point in the parameter space (denoted by the

bioRxiv preprint doi: https://doi.org/10.1101/182444; this version posted August 30, 2017. The copyright holder for this preprint (which was not certified by peer review) is the author/funder, who has granted bioRxiv a license to display the preprint in perpetuity. It is made available under aCC-BY 4.0 International license.

boundary between blue and yellow in Figure 2b), whereby small increases in σ lead to substantial alterations in the phase relationships between regions. Specifically, the network abruptly shifts from stable equilibrium to high-amplitude synchronized oscillation, facilitating an increase in effective communication between otherwise topologically distant regions (Fries, 2005; Varela et al., 2001). This same transition point is associated with a peak in informational complexity (Figure 3), further suggesting the importance of criticality in maximizing the information processing capacity of global network topology. Notably, the transition is also accompanied by a peak in the topological variability over time: hence a dynamic instability amongst fast neuronal oscillations yields increased network fluctuations at very slow time scales, again highlighting the crucial role of criticality to multi-scale neural phenomena (Cocchi et al., 2017).

The effect of neural gain on topology was greatest in a bilateral network of high-degree frontoparietal cortical regions (Figure 4). This suggests that the recruitment of these hub regions at intermediate levels of excitability and neural gain shifts collective network dynamics across a bifurcation, increasing effective interactions between otherwise segregated regions. This result underlines the effective influence of the structural 'rich club' (Figure 4), which in addition to providing topological support to the structural connectome (van den Heuvel and Sporns, 2013), may also facilitate the transition between distinct topological states. Crucially, these states have been shown to underlie effective cognitive performance (Shine et al., 2016a), episodic memory retrieval (Westphal et al., 2017) and conscious awareness (Barttfeld et al., 2015; Godwin et al., 2015), confirming the importance of ascending neuromodulatory systems for a suite of higher-level behavioral capacities.

Overall, our findings broadly support the predictions of the neural gain hypothesis of noradrenergic function (Aston-Jones and Cohen, 2005b). For instance, the relationship between neural gain and topology demonstrated an inverted-U shaped curve, providing network-level insight into the long-standing notion of a nonlinear relationship between catecholamine levels and effective cognitive performance (Robbins and Arnsten, 2009; Shine et al., 2016a; Figure 1a). In addition, our results also align with previous hypotheses that highlighted the

bioRxiv preprint doi: https://doi.org/10.1101/182444; this version posted August 30, 2017. The copyright holder for this preprint (which was not certified by peer review) is the author/funder, who has granted bioRxiv a license to display the preprint in perpetuity. It is made available under aCC-BY 4.0 International license.

importance of α2-adrenoreceptor mediated hub recruitment with increasing concentrations of noradrenaline, particularly in the frontal cortex (Robbins and Arnsten, 2009; Sara, 2009). However, our findings are inconsistent with the hypothesis that neural gain mediates an increase in tightly clustered patterns of neural interactions (Eldar et al., 2013). In contrast to this prediction, our simulations showed that measures that reflect an increase in local clustering, such as modularity and the mean clustering coefficient (Figure S4), did not increase as a function of neural gain in the same manner as other measures, such as the mean participation coefficient. Therefore, our results suggest that an increase in functional integration (and hence, a concomitant decrease in local clustering) is a more effective indicator of the topological influence of increasing neural gain. However, it bears mention that the hypothesized relationship between clustering and neural gain was presented in the context of a focused learning paradigm (Eldar et al., 2013), whereas our data were not modeled in an explicit behavioral context. As such, future studies are required to disambiguate the relative relationship between neural gain and network topology as a function of task performance.

Prior computational studies have demonstrated a link between the structural and functional connectome, with the broad repertoire of functional network dynamics bounded by structural constraints imposed by the white-matter backbone of the brain (Deco and Jirsa, 2012; Honey et al., 2007; 2009). While the targeted role of gain modulation on local neuronal dynamics have been studied (Freeman, 1979), the impact of gain on functional network activity has not been pursued. Here, we have demonstrated a putative mechanism by which a known biological system (namely, the ascending noradrenergic system) can mediate structural-functional changes, essentially by navigating the functional connectome across a topological landscape characterized by alterations in oscillatory synchrony. However, the direct relationship between neural gain manipulation and the ascending noradrenergic system is likely to represent an oversimplification. Indeed, given the complexity and hierarchical organization of the brain, it is almost certain that other functional systems, such as the thalamus (Hwang et al., 2016) and fast-spiking interneurons (Stringer et al., 2016), play significant roles in mediating neural gain and hence, the balance between

bioRxiv preprint doi: https://doi.org/10.1101/182444; this version posted August 30, 2017. The copyright holder for this preprint (which was not certified by peer review) is the author/funder, who has granted bioRxiv a license to display the preprint in perpetuity. It is made available under aCC-BY 4.0 International license.

integration and segregation. Further studies are required to interrogate these mechanisms more directly.

A somewhat surprising result of our simulation is the link between phase- and amplitude-related measures of neuronal coupling. It has been known for some time that the BOLD signal is insensitive to the relative phase of underlying neural dynamics (Foster et al., 2016), relating more closely to fluctuations in the relative amplitude of neural firing. Based on this knowledge, we can infer that estimates of connectivity using BOLD time series relate to covariance in amplitude fluctuations among pairs of regions, rather than alterations in phase synchrony. This clarification is important for modern theories of functional neuroscience, as synchronous relationships between regions in the phase domain have been used to explain effective communication between neural regions (Fries, 2015; Lisman and Jensen, 2013; Siegel et al., 2009), in which the precise timing between spiking populations determines the efficacy of information processing. Our results suggest a surprisingly robust link between these two measures, such that an integrated network with increased inter-modular amplitude correlation coincides with a peak in ordered phase synchrony between regions. In our model, the peak of network variability occurs at the critical transition between disordered and ordered phases, where the local dynamic states shows the most variability and where fast stochastic perturbations are most able to influence slow amplitude fluctuations. However, while our model provides evidence linking neural gain to functional integration, advanced models that display a broader variety of non-linear dynamics (Breakspear, 2017) are required to test these hypotheses more directly.

Together, our results suggest that the balance between integration and segregation relates to alterations in neural gain that exist within a 'zone' of maximal communicability and temporal variability. Our findings thus highlight important constraints on contemporary models of brain function, while also providing crucial implications for understanding effective brain function during task performance or as a function of neurodegenerative or psychiatric disease.

bioRxiv preprint doi: https://doi.org/10.1101/182444; this version posted August 30, 2017. The copyright holder for this preprint (which was not certified by peer review) is the author/funder, who has granted bioRxiv a license to display the preprint in perpetuity. It is made available under aCC-BY 4.0 International license.

Methods

Dynamical Network Modeling

The Virtual Brain software (Sanz Leon et al., 2013) was used to simulate neural data across a lattice of parameter points in which we manipulated the inter-regional coupling between regions using both a gain parameter and an excitability parameter. Specifically, we used a generic 2-dimensional oscillator model (Equations 1 and 2) to create time series data that represents neural activity via two variables (the membrane potential and a slow recovery variable). This equation is based upon a modal approximation (Stefanescu and Jirsa, 2008) of a population of Fitzhugh-Nagumo neurons (Izhikevich and Fitzhugh, 2006). The neuronal dynamics are given by,

$$\dot{V}_i(t) = 20(W_i(t) + 3V_i(t)^2 - V_i(t)^3 + \gamma I_i) + \xi_i(t), \quad [1]$$

$$\dot{W}_i(t) = 20\big(-W_i(t) - 10V_i(t)\big) + \eta_i(t), \quad [2]$$

where V_i represents the local mean membrane potential and Wi represents the corresponding slow recovery variable at node i. Stochastic fluctuations are introduced additively through the white noise processes η_i and ξ_i, drawn independently from Gaussian distributions with zero mean and unit variance. The synaptic current I_i arise from time-delayed input from other regions modulated in strength by the global excitability parameter γ. This input arises after the mean membrane potential V in distant nodes is converted into a firing rate via a sigmoid-shaped activation function S, and then transmitted with axonal time delays through the connectivity matrix. Hence the synaptic current at node i is given by,

$$I_i = \sum_j A_{ij}\, \mathrm{S}_j\big(t - \tau_{ij}\big) \quad [3]$$

where A_{ij} is the directed connectivity matrix derived from the 76 region CoCoMac connectome (Kötter, 2004), and τ_{ij} is the corresponding time delay computed from the length of fiber tracts estimated by diffusion spectrum imaging (Sanz Leon et al., 2013). The conversion from regional membrane potential to firing rate is given by a sigmoid-shaped activation function,

bioRxiv preprint doi: https://doi.org/10.1101/182444; this version posted August 30, 2017. The copyright holder for this preprint (which was not certified by peer review) is the author/funder, who has granted bioRxiv a license to display the preprint in perpetuity. It is made available under aCC-BY 4.0 International license.

$$S_i(t) = \frac{1}{1+ e^{-\sigma(V_i(t)-m)}}, \quad [4]$$

where σ is the (global) gain parameter and the sigmoid activation function is shifted to center at m. These equations were integrated using a stochastic Heun method (Rüemelin, 1982).

The simulated neuronal data were fed through a Balloon-Windkessel model to simulate realistic Blood Oxygen Level Dependent signals (Friston et al., 2000). The simulated BOLD time series were band-pass filtered (0.01 – 0.1 Hz) and the Pearson's correlation was then computed (and normalized using Fisher's r-to-Z transformation).

We manipulated the inter-regional neural gain parameter σ and the regional excitability γ through a range of values (between 0-1). After aligning the sensitive region of the sigmoid function with its mean input (m = 1.5). Consistent with the effects of relatively diffuse projections from the locus coeruleus to cortex, all regions were given the same values of the σ and γ parameter for each trial. All code is freely available at https://github.com/macshine/gain_topology (repository currently private).

Integration and Segregation

The Louvain modularity algorithm from the Brain Connectivity Toolbox (Rubinov and Sporns, 2010) was used to estimate time-averaged community structure. The Louvain algorithm iteratively maximizes the modularity statistic, Q, for different community assignments until the maximum possible score of Q has been obtained (Equation 5). The modularity estimate for a given network is therefore a quantification of the extent to which the network may be subdivided into communities with stronger within-module than between-module connections. Here, we used the Q parameter to estimate the extent of segregation within each graph,

$$Q = \frac{1}{v^+}\sum_{ij}\left(w_{ij}^+ - e_{ij}^+\right)\delta_{M_iM_j} - \frac{1}{v^+ + v^-}\sum_{ij}\left(w_{ij}^- - e_{ij}^-\right)\delta_{M_iM_j} \quad [5]$$

where v is the total weight of the network (sum of all negative and positive connections), w_{ij} is the weighted and signed connection between regions i and j,

bioRxiv preprint doi: https://doi.org/10.1101/182444; this version posted August 30, 2017. The copyright holder for this preprint (which was not certified by peer review) is the author/funder, who has granted bioRxiv a license to display the preprint in perpetuity. It is made available under aCC-BY 4.0 International license.

e_{ij} is the strength of a connection divided by the total weight of the network, and δ_{MiMj} is set to 1 when regions are in the same community and 0 otherwise. '+' and '–' superscripts denote all positive and negative connections, respectively. Consistent with previous work (Eldar et al., 2013), the mean clustering coefficient, which reflects the proportion of closed 'triangles' in the binarized graph, was also used as a measure of segregation (Rubinov and Sporns, 2010).

For each level of neural gain, the community assignment for each region was assessed 100 times and a consensus partition was identified using a fine-tuning algorithm from the Brain Connectivity Toolbox (http://www.brain-connectivity-toolbox.net/). All graph theoretical measures were calculated on weighted and signed connectivity matrices (Rubinov and Sporns, 2010), and weak connections were retained using a consistency thresholding technique that identifies weak, yet consistent connections by identifying edges with minimal variance across multiple iterations (Roberts et al., 2016). In order to assess global, large-scale communities, the resolution parameter was set to 1.0 (higher values tune the algorithm to detect smaller communities, which instead reflect local, rather than global, clustering). This parameter was chosen by calculating the resolution value which maximized the Surprise (Aldecoa and Marín, 2013) between the community structure of the network at each level of gain and resolution and a random network defined using a cumulative hypergeometric distribution (see Aldecoa and Marín, 2013 and Figure S3 for details).

The participation coefficient, B_A (Equation 6) quantifies the extent to which a region connects across all modules (i.e. between-module strength). As such, the mean participation coefficient can be used to estimate the extent of integration within a graph. The participation coefficient, B_{Ai}, for a given region i is,

$$B_{Ai} = 1 - \sum_{s=1}^{n_M} \left(\frac{\kappa_{is}}{\kappa_i}\right)^2 \quad [6]$$

where κ_{is} is the strength of the positive connections of region i to regions in module s, and κ_i is the sum of strengths of all positive connections of region i. The participation coefficient of a region is therefore close to 1 if its connections are uniformly distributed among all the modules and 0 if all of its links are within its own module.

bioRxiv preprint doi: https://doi.org/10.1101/182444; this version posted August 30, 2017. The copyright holder for this preprint (which was not certified by peer review) is the author/funder, who has granted bioRxiv a license to display the preprint in perpetuity. It is made available under aCC-BY 4.0 International license.

Phase Synchrony Order Parameter

To estimate the degree of phase synchrony at different points in the parameter space, we extracted the raw signal from each region in the simulation and subtracted the least squares linear trend from each channel. We then computed the phase of the analytic signal for each channel using the Hilbert transform and then estimated the phase synchrony order parameter (across all channels), OP, which is given by,

$$\rho = \left| \frac{1}{N} \sum_{j=1}^{N} e^{i\theta_j} \right| \quad [7]$$

where $i = \sqrt{-1}$ and θ_j represents the oscillation phase of the j^{th} region. Large values of ρ denote phase alignment between regions (Breakspear and Heitmann, 2010; Kuramoto, 1984). The value of ρ for each parameter combination was subsequently averaged over time and across sessions. By designating each parameter combination as resulting in either a synchronized ($\rho \geq 0.5$) or unsynchronized ($\rho < 0.5$) regime, we were able to determine whether network topology changes as a function of neural gain and excitability estimated from BOLD data coincided with changes of underlying phase synchrony. Specifically, we then separately grouped topological variables and within- and between-hemisphere connectivity according to their underlying ρ value and then estimated an independent-samples t-test between the two groups.

Communicability

The communicability between a pair of nodes is defined as a weighted sum of the number of all walks connecting the pair of nodes and has been shown to be equivalent to the matrix exponent of a binarized graph (Estrada and Hatano, 2008). For ease of interpretation, we calculated the $\log_{10}$-transformed mean of communicability for each graph across iterations and values of neural gain.

Topological Variability

To estimate time-resolved functional connectivity between the 76 nodal pairs, we used a recently described statistical technique (Multiplication of Temporal Derivatives; Shine et al., 2015; http://github.com/macshine/coupling), which is computed by calculating the point-wise product of temporal derivative of

bioRxiv preprint doi: https://doi.org/10.1101/182444; this version posted August 30, 2017. The copyright holder for this preprint (which was not certified by peer review) is the author/funder, who has granted bioRxiv a license to display the preprint in perpetuity. It is made available under aCC-BY 4.0 International license.

pairwise time series (Equation 7). To reduce the contamination of high-frequency noise in the time-resolved connectivity data, M_{ij} was averaged over a temporal window (w = 15 time points). Individual functional connectivity matrices were calculated within each temporal window, thus generating an unthresholded (signed and weighted) 3D adjacency matrix (region × region × time) for each participant. These matrices were then subjected to time-resolved topological analyses, which allowed us to estimate the participation coefficient for each region over time (B_T). We used the mean regional standard deviation of this measure to estimate time-resolved topological variability in the simulated data.

$$M_{ijt} = \frac{1}{w}\sum_{t}^{t+w} \frac{(dt_{it} \times dt_{jt})}{(\sigma_{dt_i} \times \sigma_{dt_j})} \quad [8]$$

for each time point, t, M_{ij} is defined according to equation 1, where dt is the first temporal derivative of the i^{th} or j^{th} time series at time t, σ is the standard deviation of the temporal derivative time series for region i or j and w is the window length of the simple moving average. This equation can then be calculated over the course of a time series to obtain an estimate of time-resolved connectivity between pairs of regions.

Structural Rich Club

To test whether changes associated with neural gain were mediated by highly-interconnected high-degree hubs, we identified a set of 'rich club' regions using the structural white matter connectome from the CoCoMac database (Kötter, 2004). Briefly, the degree of each node i in the network was determined by calculating the number of links that node i shared with k other nodes in the network. All nodes that showed a number of connections of $\leq k$ were removed from the network. For the remaining network, the rich-club coefficient (Φ_k) was computed as the ratio of connections present between the remaining nodes and the total number of possible connections that would be present when the set would be fully connected. We then normalized Φ_k relative to a set of random networks with similar density and connectivity distributions. When Φ_Z is greater than 1, the network can be said to display a 'rich club' architecture. Individual regions that are interconnected at the value of k at which the network demonstrates a 'rich club' architecture are thus designated as 'rich club' nodes (n

bioRxiv preprint doi: https://doi.org/10.1101/182444; this version posted August 30, 2017. The copyright holder for this preprint (which was not certified by peer review) is the author/funder, who has granted bioRxiv a license to display the preprint in perpetuity. It is made available under aCC-BY 4.0 International license.

= 22). Any nodes outside of this group but still sharing a connection are labeled as 'feeder' nodes (n = 44), and regions disconnected from the rich club are designated as 'local' nodes (n = 10). The results were projected onto a standard surface representation of the macaque cortex (Figure 4). After segmenting the network in this fashion, we were able to estimate the realized mean gain and B_A across the parameter space for regions according to their structural topology.

Realized Neural Gain

While the neural gain parameter σ controls the *maximum* gain in each region within the simulation by setting the maximum slope of the sigmoid, the realized gain (mean ratio of sigmoid output to input) for each brain region depends upon the distribution of its input, and is greater when the input level is concentrated near the center of the sigmoid. We estimated the regional variation in effective or 'realized' neural gain by calculating the integral of the instantaneous sigmoid slope over its complete input range, weighted by the probability of each input level. We then compared these values as a function of nodal class (rich club vs other nodes) at each aspect of the parameter space.

Reliability

We ran a number of subsequent tests to ensure that any observed changes in network topology were robust to the processing steps utilized in the analysis. Firstly, we re-analyzed data across a range of network thresholds (1-20%) and observed robust results (i.e. $r > 0.75$) for Q, mean B_A, mean communicability and the standard deviation of B_T on graphs estimated between the 9-20% threshold range. Secondly, as the number of modules estimated from graphs can change as a function of network topology, we re-examined the topological characteristics of networks that were matched for the number of modules (N = 4) and found no significant differences to the topological signatures estimated on the whole group.

bioRxiv preprint doi: https://doi.org/10.1101/182444; this version posted August 30, 2017. The copyright holder for this preprint (which was not certified by peer review) is the author/funder, who has granted bioRxiv a license to display the preprint in perpetuity. It is made available under aCC-BY 4.0 International license.

Supplementary Figures

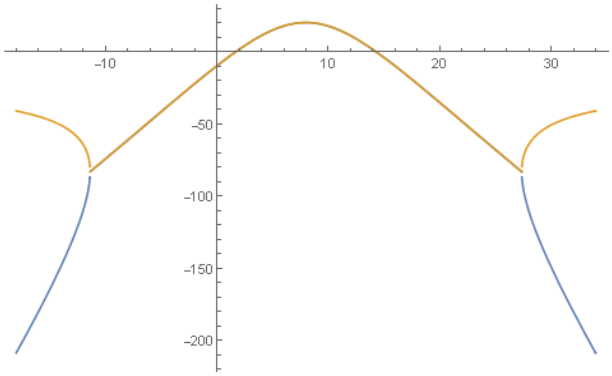

Figure S1 – Transition to self-sustained oscillations in a single brain region. For the generic 2D oscillator model this shows the real parts of eigenvalues at equilibrium as the level of input (I_{app}) to a region is increased. A transition to self-sustained oscillations in a local region occurs where this curve crosses zero. That regime is bounded by supercritical Hopf bifurcations at $I_{app} = 2.0$ and $I_{app} = 14$.

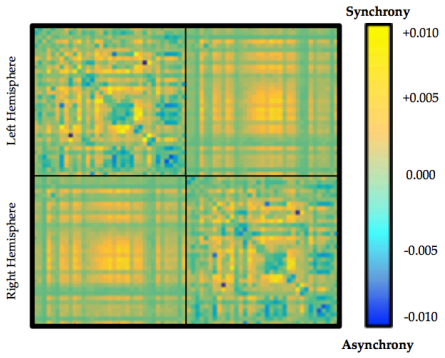

Figure S2 – Average time-averaged connectivity matrix in regions of the parameter space associated with high (yellow) or low (blue) ordered phase synchrony.

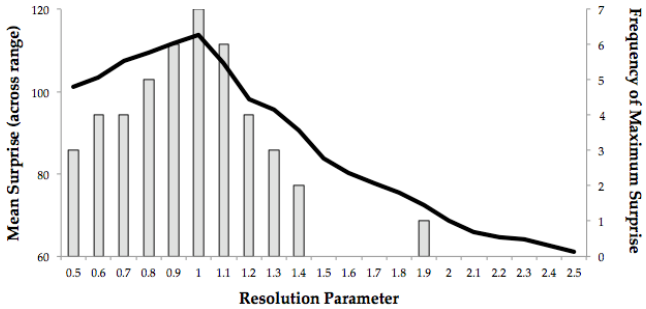

Figure S3 – Parameter choice using Surprise (Aldecoa and Marín, 2013) maximization across different levels of gamma: the line plot demonstrates the mean value of Surprise across the range of gamma across the range of gain parameters; the column plot displays a histogram denoting the instance of the maximum value of Surprise at each particular level of gain. Both the mean and summed maximum plots demonstrate a peak level of Surprise at resolution = 1.0.

bioRxiv preprint doi: https://doi.org/10.1101/182444; this version posted August 30, 2017. The copyright holder for this preprint (which was not certified by peer review) is the author/funder, who has granted bioRxiv a license to display the preprint in perpetuity. It is made available under aCC-BY 4.0 International license.

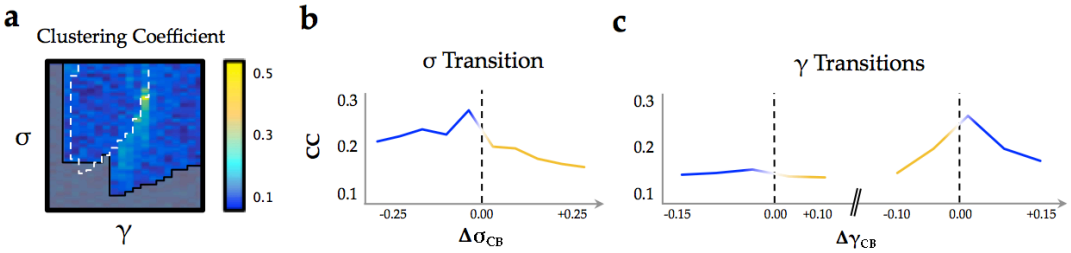

Figure S4 – Clustering coefficient: a) clustering coefficient across the parameter space; b) as a function of changes in neural gain; and c) excitability.

bioRxiv preprint doi: https://doi.org/10.1101/182444; this version posted August 30, 2017. The copyright holder for this preprint (which was not certified by peer review) is the author/funder, who has granted bioRxiv a license to display the preprint in perpetuity. It is made available under aCC-BY 4.0 International license.

698 **Author Contributions**

699 JMS and RP conceived of the study and performed the initial analyses. MA and
700 MB performed subsequent simulation and analysis of the network model. JMS
701 wrote the first draft. All authors provided feedback on the final draft.

702

703 **Acknowledgements**

704 We thank the creators of the Virtual Brain for their open-source software, Peter
705 Bell for helpful comments, Bratislav Misic for sharing code and Joke Durnez for
706 statistical advice.

707

708

709

710

711

712

713

714

715

716

717

718

719

720

721

722

723

724

725

726

727

728

729

730

731

732

bioRxiv preprint doi: https://doi.org/10.1101/182444; this version posted August 30, 2017. The copyright holder for this preprint (which was not certified by peer review) is the author/funder, who has granted bioRxiv a license to display the preprint in perpetuity. It is made available under aCC-BY 4.0 International license.

References

Aldecoa, R., Marín, I., 2013. Surprise maximization reveals the community structure of complex networks. Sci Rep 3, 1060. doi:10.1038/srep01060

Aston-Jones, G., Cohen, J.D., 2005a. An integrative theory of locus coeruleus-norepinephrine function: adaptive gain and optimal performance. Annu. Rev. Neurosci. 28, 403–450. doi:10.1146/annurev.neuro.28.061604.135709

Aston-Jones, G., Cohen, J.D., 2005b. An Integrative Theory of Locus Coeruleus-Norepinephrine Function: Adaptive Gain and Optimal Performance. Annu. Rev. Neurosci. 28, 403–450.

Barttfeld, P., Uhrig, L., Sitt, J.D., Sigman, M., Jarraya, B., Dehaene, S., 2015. Signature of consciousness in the dynamics of resting-state brain activity. Proc. Natl. Acad. Sci. U.S.A. 112, 887–892. doi:10.1073/pnas.1418031112

Bassett, D.S., Yang, M., Wymbs, N.F., Grafton, S.T., 2015. Learning-induced autonomy of sensorimotor systems. Nat Neurosci 18, 744–751. doi:10.1038/nn.3993

Breakspear, M., 2017. Dynamic models of large-scale brain activity. Nat Neurosci 20, 340–352. doi:10.1038/nn.4497

Breakspear, M., Heitmann, S., 2010. Generative models of cortical oscillations: neurobiological implications of the Kuramoto model. Front Hum Neurosci 4, 190.

Bullmore, E., Sporns, O., 2012. The economy of brain network organization. Nat. Rev. Neurosci. 13, 336–349. doi:10.1038/nrn3214

Chang, C., Glover, G.H., 2010. Time-frequency dynamics of resting-state brain connectivity measured with fMRI. NeuroImage 50, 81–98. doi:10.1016/j.neuroimage.2009.12.011

Chialvo, D.R., 2010. Emergent complex neural dynamics. Nature physics 6, 744–750.

Cocchi, L., Gollo, L.L., Zalesky, A., Breakspear, M., 2017. Criticality in the brain: A synthesis of neurobiology, models and cognition. Progress in Neurobiology Ahead of Print.

Deco, G., Jirsa, V., McIntosh, A.R., Sporns, O., Kötter, R., 2009. Key role of coupling, delay, and noise in resting brain fluctuations. Proc. Natl. Acad. Sci. U.S.A. 106, 10302–10307. doi:10.1073/pnas.0901831106

Deco, G., Jirsa, V.K., 2012. Ongoing cortical activity at rest: criticality, multistability, and ghost attractors. J. Neurosci. 32, 3366–3375. doi:10.1523/JNEUROSCI.2523-11.2012

Deco, G., Jirsa, V.K., McIntosh, A.R., 2013. Resting brains never rest: computational insights into potential cognitive architectures. Trends in Neurosciences 36, 268–274. doi:10.1016/j.tins.2013.03.001

Deco, G., Kringelbach, M.L., Jirsa, V.K., Ritter, P., 2017. The dynamics of resting

bioRxiv preprint doi: https://doi.org/10.1101/182444; this version posted August 30, 2017. The copyright holder for this preprint (which was not certified by peer review) is the author/funder, who has granted bioRxiv a license to display the preprint in perpetuity. It is made available under aCC-BY 4.0 International license.

773 fluctuations in the brain: metastability and its dynamical cortical core. Sci
774 Rep 7, 3095. doi:10.1038/s41598-017-03073-5
775 Deco, G., Tononi, G., Boly, M., Kringelbach, M.L., 2015a. Rethinking segregation
776 and integration: contributions of whole-brain modelling. Nat. Rev. Neurosci.
777 16, 430–439. doi:10.1038/nrn3963
778 Deco, G., Tononi, G., Boly, M., Kringelbach, M.L., 2015b. Rethinking segregation
779 and integration: contributions of whole-brain modelling. Nat. Rev. Neurosci.
780 16, 430–439. doi:10.1038/nrn3963
781 Eldar, E., Cohen, J.D., Niv, Y., 2013. The effects of neural gain on attention and
782 learning. Nat Neurosci 16, 1146-53.
783 Estrada, E., Hatano, N., 2008. Communicability in complex networks. Phys Rev E
784 Stat Nonlin Soft Matter Phys 77, 036111. doi:10.1103/PhysRevE.77.036111
785 Fitzhugh, R., 1961. Impulses and Physiological States in Theoretical Models of
786 Nerve Membrane. Biophys. J. 1, 445–466.
787 Foster, B.L., He, B.J., Honey, C.J., Jerbi, K., 2016. Spontaneous Neural Dynamics
788 and Multi-scale Network Organization. Frontiers in Systems Neuroscience
789 10, 7.
790 Freeman, W.J., 1979. Nonlinear gain mediating cortical stimulus-response
791 relations. Biol Cybern 33, 237–247.
792 Fries, P., 2015. Rhythms for Cognition: Communication through Coherence.
793 Neuron 88, 220–235. doi:10.1016/j.neuron.2015.09.034
794 Fries, P., 2005. A mechanism for cognitive dynamics: neuronal communication
795 through neuronal coherence. Trends in Cognitive Sciences 9, 474–480.
796 doi:10.1016/j.tics.2005.08.011
797 Friston, K.J., Mechelli, A., Turner, R., Price, C.J., 2000. Nonlinear responses in
798 fMRI: the Balloon model, Volterra kernels, and other hemodynamics.
799 NeuroImage 12, 466-477.
800 Ghosh, A., Rho, Y., McIntosh, A.R., Kotter, R., Jirsa, V.K., 2008. Noise during Rest
801 Enables the Exploration of the Brain's Dynamic Repertoire. PLoS Comput.
802 Biol. 4, e1000196. doi:10.1371/journal.pcbi.1000196
803 Godwin, D., Barry, R.L., Marois, R., 2015. Breakdown of the brain's functional
804 network modularity with awareness. Proc. Natl. Acad. Sci. U.S.A. 112, 3799–
805 3804. doi:10.1073/pnas.1414466112
806 Gollo, L.L., Zalesky, A., Hutchison, R.M., van den Heuvel, M., Breakspear, M.,
807 2015. Dwelling quietly in the rich club: brain network determinants of slow
808 cortical fluctuations. Philosophical Transactions of the Royal Society B:
809 Biological Sciences 370, 20140165–20140165. doi:10.1098/rstb.2014.0165
810 Honey, C.J., Kotter, R., Breakspear, M., Sporns, O., 2007. Network structure of
811 cerebral cortex shapes functional connectivity on multiple time scales.
812 Proceedings of the National Academy of Sciences 104, 10240–10245.

bioRxiv preprint doi: https://doi.org/10.1101/182444; this version posted August 30, 2017. The copyright holder for this preprint (which was not certified by peer review) is the author/funder, who has granted bioRxiv a license to display the preprint in perpetuity. It is made available under aCC-BY 4.0 International license.

doi:10.1073/pnas.0701519104

Honey, C.J., Sporns, O., Cammoun, L., Gigandet, X., Thiran, J.P., Meuli, R., Hagmann, P., 2009. Predicting human resting-state functional connectivity from structural connectivity. Proceedings of the National Academy of Sciences 106, 2035–2040. doi:10.1073/pnas.0811168106

Hutchison, R.M., Womelsdorf, T., Allen, E.A., Bandettini, P.A., Calhoun, V.D., Corbetta, M., Penna, Della, S., Duyn, J.H., Glover, G.H., Gonzalez-Castillo, J., Handwerker, D.A., Keilholz, S., Kiviniemi, V., Leopold, D.A., de Pasquale, F., Sporns, O., Walter, M., Chang, C., 2013. Dynamic functional connectivity: Promise, issues, and interpretations. NeuroImage 80, 360–378. doi:10.1016/j.neuroimage.2013.05.079

Hwang, K., Bertolero, M.A., Liu, W., D'Esposito, M., 2016. The human thalamus is an integrative hub for functional brain networks. Journal of Neuroscience 37, 5594-5607.

Izhikevich, E.M., Fitzhugh, R., 2006. Fitzhugh-nagumo model. Scholarpedia.

Jirsa, V.K., Sporns, O., Breakspear, M., Deco, G., McIntosh, A.R., 2010. Towards the virtual brain: network modeling of the intact and the damaged brain. Arch Ital Biol 148, 189–205.

Joshi, S., Li, Y., Kalwani, R.M., Gold, J.I., 2016. Relationships between Pupil Diameter and Neuronal Activity in the Locus Coeruleus, Colliculi, and Cingulate Cortex. Neuron 89, 221–234. doi:10.1016/j.neuron.2015.11.028

Kötter, R., 2004. Online retrieval, processing, and visualization of primate connectivity data from the CoCoMac database. NI 2, 127–144. doi:10.1385/NI:2:2:127

Kuramoto, Y., 1984. Chemical oscillations, waves, and turbulence. Springer.

Lisman, J.E., Jensen, O., 2013. The θ-γ neural code. Neuron 77, 1002–1016. doi:10.1016/j.neuron.2013.03.007

Mišić, B., Betzel, R.F., Nematzadeh, A., Goñi, J., Griffa, A., Hagmann, P., Flammini, A., Ahn, Y.-Y., Sporns, O., 2015. Cooperative and Competitive Spreading Dynamics on the Human Connectome. Neuron 86, 1518–1529. doi:10.1016/j.neuron.2015.05.035

Murphy, P.R., O'Connell, R.G., O'Sullivan, M., Robertson, I.H., Balsters, J.H., 2014. Pupil diameter covaries with BOLD activity in human locus coeruleus. Hum Brain Mapp 35, 4140–4154. doi:10.1002/hbm.22466

Park, H.-J., Friston, K., 2013. Structural and Functional Brain Networks: From Connections to Cognition. Science 342, 1238411–1238411. doi:10.1126/science.1238411

Reimer, J., Froudarakis, E., Cadwell, C.R., Yatsenko, D., Denfield, G.H., Tolias, A.S., 2014. Pupil Fluctuations Track Fast Switching of Cortical States during Quiet Wakefulness. Neuron 84, 355–362. doi:10.1016/j.neuron.2014.09.033

bioRxiv preprint doi: https://doi.org/10.1101/182444; this version posted August 30, 2017. The copyright holder for this preprint (which was not certified by peer review) is the author/funder, who has granted bioRxiv a license to display the preprint in perpetuity. It is made available under aCC-BY 4.0 International license.

853 Reimer, J., McGinley, M.J., Liu, Y., Rodenkirch, C., Wang, Q., McCormick, D.A.,
854 Tolias, A.S., 2016. Pupil fluctuations track rapid changes in adrenergic and
855 cholinergic activity in cortex. Nat Commun 7, 13289.
856 doi:10.1038/ncomms13289
857 Robbins, T.W., Arnsten, A.F.T., 2009. The Neuropsychopharmacology of Fronto-
858 Executive Function: Monoaminergic Modulation. Annu. Rev. Neurosci. 32,
859 267–287. doi:10.1146/annurev.neuro.051508.135535
860 Roberts, J.A., Perry, A., Roberts, G., Mitchell, P.B., Breakspear, M., 2016.
861 Consistency-based thresholding of the human connectome. NeuroImage 145,
862 118-129.
863 Rubinov, M., Sporns, O., 2010. Complex network measures of brain connectivity:
864 Uses and interpretations. NeuroImage 52, 1059–1069.
865 doi:10.1016/j.neuroimage.2009.10.003
866 Rüemelin, W., 1982. Numerical Treatment of Stochastic Differential Equations.
867 SIAM J. Numer. Anal. 19, 604–613. doi:10.1137/0719041
868 Sanz Leon, P., Knock, S.A., Woodman, M.M., Domide, L., Mersmann, J.,
869 McIntosh, A.R., Jirsa, V., 2013. The Virtual Brain: a simulator of primate brain
870 network dynamics. Front Neuroinform 7, 10. doi:10.3389/fninf.2013.00010
871 Sara, S.J., 2009. The locus coeruleus and noradrenergic modulation of cognition.
872 Nat. Rev. Neurosci. 10, 211–223. doi:10.1038/nrn2573
873 Servan-Schreiber, D., Printz, H., Cohen, J., 1990. A network model of
874 catecholamine effects- Gain, signal-to-noise ratio, and behavior. Science 249,
875 892-895.
876 Shine, J.M., Bissett, P.G., Bell, P.T., Koyejo, O., Balsters, J.H., Gorgolewski, K.J.,
877 Moodie, C.A., Poldrack, R.A., 2016a. The Dynamics of Functional Brain
878 Networks: Integrated Network States during Cognitive Task Performance.
879 Neuron 92, 544–554. doi:10.1016/j.neuron.2016.09.018
880 Shine, J.M., Koyejo, O., Bell, P.T., Gorgolewski, K.J., Gilat, M., Poldrack, R.A.,
881 2015. Estimation of dynamic functional connectivity using Multiplication of
882 Temporal Derivatives. NeuroImage 122, 399–407.
883 Shine, J.M., Koyejo, O., Poldrack, R.A., 2016b. Temporal metastates are associated
884 with differential patterns of time-resolved connectivity, network topology,
885 and attention. Proc. Natl. Acad. Sci. U.S.A. 113, 9888–9891.
886 doi:10.1073/pnas.1604898113
887 Siegel, M., Warden, M.R., Miller, E.K., 2009. Phase-dependent neuronal coding of
888 objects in short-term memory. Proc. Natl. Acad. Sci. U.S.A. 106, 21341–21346.
889 doi:10.1073/pnas.0908193106
890 Sporns, O., 2013. The human connectome: origins and challenges. NeuroImage
891 80, 53–61. doi:10.1016/j.neuroimage.2013.03.023
892 Stefanescu, R.A., Jirsa, V.K., 2011. Reduced representations of heterogeneous

bioRxiv preprint doi: https://doi.org/10.1101/182444; this version posted August 30, 2017. The copyright holder for this preprint (which was not certified by peer review) is the author/funder, who has granted bioRxiv a license to display the preprint in perpetuity. It is made available under aCC-BY 4.0 International license.

mixed neural networks with synaptic coupling. Phys Rev E Stat Nonlin Soft Matter Phys 83, 026204. doi:10.1103/PhysRevE.83.026204

Stefanescu, R.A., Jirsa, V.K., 2008. A Low Dimensional Description of Globally Coupled Heterogeneous Neural Networks of Excitatory and Inhibitory Neurons. PLoS Comput. Biol. 4, e1000219. doi:10.1371/journal.pcbi.1000219

Stringer, C., Pachitariu, M., Steinmetz, N.A., Okun, M., Bartho, P., Harris, K.D., Sahani, M., Lesica, N.A., 2016. Inhibitory control of correlated intrinsic variability in cortical networks. Elife 5, 91. doi:10.7554/eLife.19695

Tononi, G., Sporns, O., 1994. A measure for brain complexity: relating functional segregation and integration in the nervous system. Proc. Natl. Acad. Sci. U.S.A. 91, 5033–5037.

van den Heuvel, M.P., Sporns, O., 2013. An anatomical substrate for integration among functional networks in human cortex. J. Neurosci. 33, 14489–14500. doi:10.1523/JNEUROSCI.2128-13.2013

Varela, F., Lachaux, J.-P., Rodriguez, E., Martinerie, J., 2001. The brainweb: Phase synchronization and large-scale integration. Nat. Rev. Neurosci. 2, 229–239. doi:10.1038/35067550

Waterhouse, B.D., Sessler, F.M., Jung-Tung, C., 1988. New evidence for a gating action of norepinephrine in central neuronal circuits of mammalian brain. Brain Research 21, 425-432.

Westphal, A.J., Wang, S., Rissman, J., 2017. Episodic memory retrieval benefits from a less modular brain network organization. Journal of Neuroscience 37, 3523–3531.

Woolrich, M.W., Stephan, K.E., 2013. Biophysical network models and the human connectome. NeuroImage 80, 330–338. doi:10.1016/j.neuroimage.2013.03.059

Zalesky, A., Fornito, A., Cocchi, L., Gollo, L.L., Breakspear, M., 2014. Time-resolved resting-state brain networks. Proceedings of the National Academy of Sciences 111, 10341–10346. doi:10.1073/pnas.1400181111